

BROOKHAVEN NATIONAL LABORATORY

---

October 1990

---

BNL--45339

DE91 004797

# THERMAL MODELS OF ULTRARELATIVISTIC HEAVY ION COLLISIONS

**H. Von Gersdorff**Physics Department  
Brookhaven National Laboratory  
Upton, New York 11973

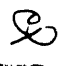
## ABSTRACT

Single-particle pseudorapidity, rapidity and transverse momentum distributions of secondaries produced in nucleus-nucleus central collisions at 14.6 and 200 A GeV are analysed using the isotropic fireball, Boltzmann and hydrodynamical models. Calculations using a transverse hydrodynamical model with a first order phase transition in the equation of state from quark-gluon plasma to final state hadrons are compared to experimental transverse momentum spectra.

Invited talk presented at  
Nuclear Physics Conference  
Caxambu, Brazil, September 3 - 5, 1990

---

This manuscript has been authored under contract number DE-AC02-76CH00016 with the U.S. Department of Energy. Accordingly, the U.S. Government retains a non-exclusive, royalty-free license to publish or reproduce the published form of this contribution, or allow others to do so, for U.S. Government purposes.

**MASTER**DISTRIBUTION OF THIS DOCUMENT IS UNLIMITED 

# THERMAL MODELS OF ULTRARELATIVISTIC HEAVY ION COLLISIONS

Henrique Prado VON GERSDORFF

Brookhaven National Laboratory, Physics Department, Upton, N.Y., 11973

Single-particle pseudorapidity, rapidity and transverse momentum distributions of secondaries produced in nucleus-nucleus central collisions at 14.6 and 200 A GeV are analysed using the isotropic fireball, Boltzmann and hydrodynamical models. Calculations using a transverse hydrodynamical model with a first order phase transition in the equation of state from quark-gluon plasma to final state hadrons are compared to experimental transverse momentum spectra.

## I. Introduction

When heavy ions collide at energies above 1 A GeV (or GeV/nucleon) a large number of particles are produced. The underlying mechanism behind this production is a two-step process: first, a fireball of highly excited hadronic matter is generated. Subsequently, it breaks up into the observed final state hadrons. This break up may be gradual or extremely fast depending on several initial factors such as the size of the fireball, its energy density, how much nuclear transparency is present, the rates of the reaction kinetics within the dense nuclear environment and so forth. If the kinetic energy of the incident nucleus is sufficiently randomized and equipartitioned among the constituent particles of the fireball, so that the entropy of the system reaches a maximum, thermodynamic equilibrium is established and a unique temperature parameter can be unambiguously attributed to the system as a whole. Furthermore, if the mean free path of these constituent particles is small compared to the nuclear radius one is justified in using relativistic hydrodynamics to characterize the systems expansion and consequent cooling. Modeling the full dynamical evolution of the system, from initial formation to final decoupling and fragmentation, is then tremendously simplified.

In this paper, we will explore, within the context of specific models, the consequences of assuming that the above conditions are established in central heavy ion collisions<sup>1</sup>(chemical equilibrium among particle species will also be assumed). We start, in section II, by comparing pseudorapidity distributions obtained by the KLM collaboration<sup>2</sup> and E802 collaboration<sup>3</sup> to models that use thermalized distribution functions to calculate particle spectra. Then, in section III, we employ relativistic hydrodynamics to compute transverse momentum distributions and compare these to NA35 data,<sup>4</sup> in search for evidence of collective flow behavior. Finally, in section IV, we briefly list and summarize the main points of this analysis.

---

This manuscript has been authored under contract number DE-AC02-76CH00016 with the U.S. Department of Energy.

## II. Thermalized fireball models for $dN/dy$ distributions

Single-particle pseudorapidity distributions are one of the main global observables of high-energy collisions. Recall that the definition of pseudorapidity  $\eta$  is

$$\eta = \frac{1}{2} \ln \left( \frac{p + p_z}{p - p_z} \right) = -\ln(\tan(\theta/2)) \quad (1)$$

where  $p_z$  and  $\theta$  are the longitudinal momentum and angle with respect to the incident projectile direction, respectively. It is thus a straightforward quantity to measure, but clearly not a Lorentz invariant one. Rapidity  $y$ , on the other hand, is defined by

$$y = \frac{1}{2} \ln \left( \frac{E + p_z}{E - p_z} \right) = \tanh^{-1}(\beta_{\parallel}) \quad (2)$$

where  $E$  is the total energy of the particle and  $\beta_{\parallel}$  its velocity along the beam axis. This quantity is much harder to measure than pseudorapidity, but has the advantage of being additive under Lorentz boosts ( $c = 1$ ). For massless particles  $\eta = y$ . For massive particles the difference between  $\eta$  and  $y$  is  $\eta - y \simeq \ln(m_T/p_T)$ , where  $m_T = \sqrt{p_T^2 + m_{\pi}^2}$ . For pions on average  $\eta - y \simeq 0.07$ , since their average transverse momentum is  $\langle p_T \rangle \simeq 350 \text{ MeV}/c$ . This difference is therefore significant only for low  $p_T$  pions. It is of course quite large for kaons and protons. Caution must be exercised thus when we interchange these variables.

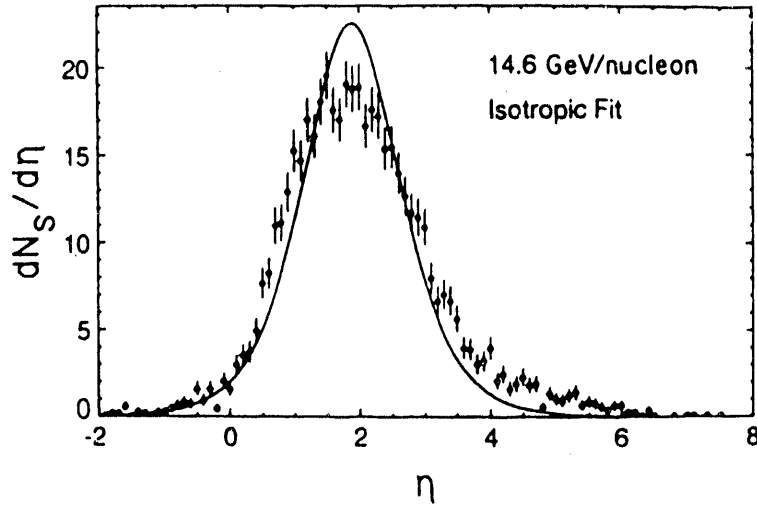


**Figure 1:** The charged particle pseudorapidity distribution for O + AgBr central collisions at 14.6 A GeV averaged over 107 events. The solid line is the best fit for the isotropic fireball model, Eq. (5), with normalized chi-square  $\chi^2 = 6.35$  for the range  $0.0 \leq \eta \leq 5.0$ . Only statistical errors are shown.

In Fig. 1 we show the KLM pseudorapidity distribution for 14.6 A GeV  $^{16}\text{O}$  projectiles incident on  $^{107}\text{Ag}^{80}\text{Br}$  emulsions, which serve both as target and  $4\pi$  solid angle detectors.<sup>2</sup> This distribution was obtained by averaging over 107 low impact parameter events, where all the polar angles  $\theta$  of charged secondaries  $N_s$  (shower particles) were measured using microscopes. In Fig. 2 the pseudorapidity distribution at 200 A GeV averaged over the 31 highest multiplicity events ( $N_s \geq 208$ ) is shown. It can be seen immediately that the distributions do

not exhibit a wide midrapidity plateau. The application of Bjorken's scaling-hydrodynamic model<sup>5</sup> to the 200 A GeV data is thus limited to particles within a one-unit rapidity window centered around midrapidity, where the 200 A GeV distribution is approximately flat. Complete transparency of the colliding nuclei is thus not present at these energies and must await the much higher center-of-mass energies of RHIC.

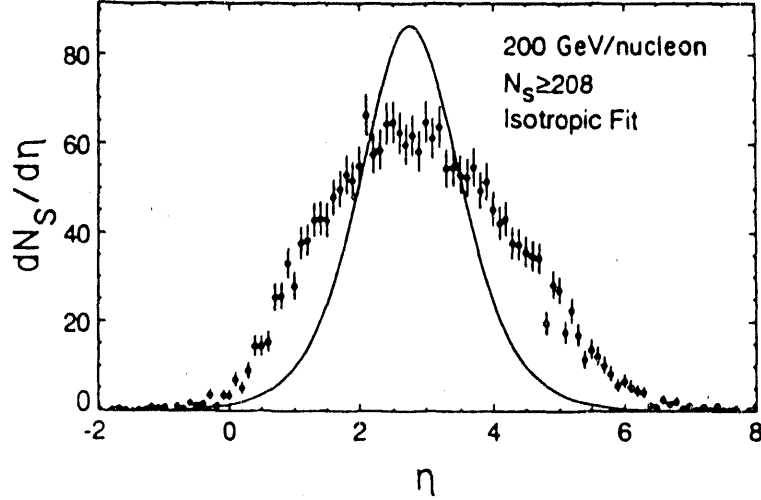


**Figure 2:** The charged particle pseudorapidity distribution for O + AgBr central collisions at 200 A GeV averaged over 31 of events with  $N_s \leq 208$ . The solid line is the best fit for the isotropic fireball model, Eq. (5), with normalized chi-square  $\chi^2 = 28.2$  for the range  $0.0 \leq \eta \leq 6.0$ . Only statistical errors are shown.

Another extreme model we may consider is a single fireball formed at midrapidity which subsequently explodes, spraying out particles isotropically in its own rest frame. In that frame the angular distribution is

$$\frac{dN_s}{d\Omega_F} = \frac{N_s}{4\pi} \quad (3)$$

which becomes, in terms of pseudorapidity,

$$\frac{dN_s}{d\eta_F} = \frac{N_s}{2} \frac{1}{[\cosh(\eta_F)]^2} \quad (4)$$

In the laboratory frame (assuming massless particles)

$$\frac{dN_s}{d\eta} = \frac{N_s}{2} \frac{1}{[\cosh(\eta - y_F)]^2} \quad (5)$$

where  $y_F = \tanh^{-1} v_F$  is the fireball rapidity and  $v_F$  its velocity in the laboratory frame. A good approximation to an isotropic distribution is a Gaussian with a width  $\delta \simeq 0.88$ ,

$$\frac{dN_s}{d\eta} \simeq \frac{N_s}{(2\pi\delta^2)^{1/2}} \exp\left[-\frac{(\eta - y_F)^2}{2\delta^2}\right] \quad (6)$$

This distribution has a constant energy-independent full width at half its maximum value  $\Delta\eta_{FWHM} = 1.75$ . A best chi-square fit to the functional form Eq. (5) is shown in Figs.

1 and 2. An isotropic fireball is thus roughly consistent with the 14.6 A GeV data, but is definitely ruled out for higher energies. Since the data show a marked monotonic increase of  $\Delta\eta_{FWHM}$  with energy we consider the roughly good fit at 14.6 A GeV to be only an accident.

We have also fit these distributions to Gaussian functions

$$\frac{dN_s}{d\eta} = \frac{N_s}{(2\pi\sigma^2)^{1/2}} \exp\left[-\frac{(\eta - \eta_0)^2}{2\sigma^2}\right] \quad (7)$$

and obtained much better fits with the width  $\sigma$  equal to  $1.02 \pm 0.03$ ,  $1.33 \pm 0.02$  and  $1.51 \pm 0.02$  for 14.6, 60 and 200 A GeV, respectively. In Fig. 3 we show the fit for the 200 A GeV high multiplicity sample of events. In Landau's hydrodynamical model<sup>6</sup> which assumes the initial hadronic matter is stopped by shock waves traversing it (full stopping), a Gaussian is obtained under suitable approximations. This model assumes the matter of the initial fireball has an equation of state of the form  $P = c_0^2 \epsilon$ , where  $P$  is the pressure,  $\epsilon$  the energy density, and  $c_0$  is the (constant) speed of sound. For  $c_0^2 = 1/3$  (an ideal relativistic Stephan-Boltzmann gas) one gets  $\sigma_L^2 = \ln(\gamma_{c.m.})$ , where  $\gamma_{c.m.}$  is the Lorentz contraction factor in the projectile-target center-of-mass frame, assuming  $A + A$  collisions (the effects of spectator nucleons are completely ignored). One thus get  $\sigma_L$  equal to 1.03, 1.31 and 1.53 for 14.6, 60 and 200 A GeV, respectively, which is in good agreement with our previous fits to data. This model is thus, at least with respect to  $dN/d\eta$ , consistent with this data.

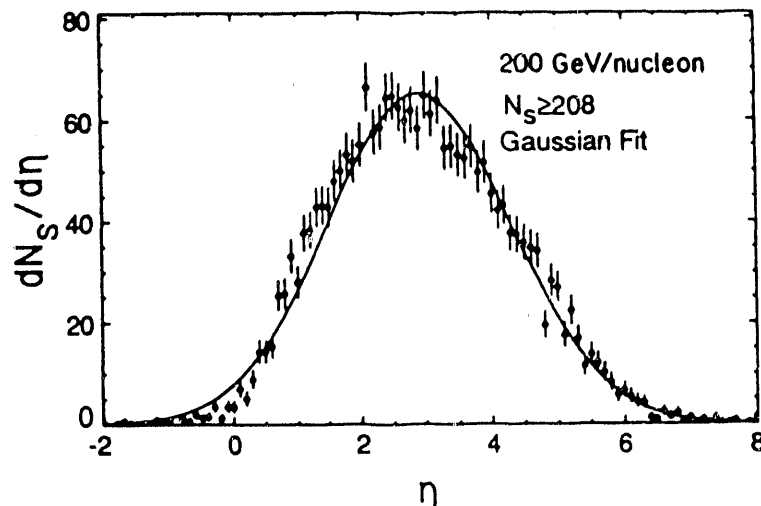


**Figure 3:** The charged particle pseudorapidity distribution for O + AgBr central collisions at 200 A GeV averaged over 31 of events with  $N_s \leq 208$ . The solid line is the best fit for a Gaussian, Eq.(7), with normalized chi-square  $\chi^2 = 2.14$  for the range  $0.0 \leq \eta \leq 6.0$ . Only statistical errors are shown.

Before leaving the subject of rapidity distributions it is instructive to consider one more thermal fireball model<sup>7</sup>, the relativistic Boltzmann gas model<sup>8</sup>. First, let's define a particle four-flow vector

$$N^\mu(x) = \int \frac{d^3p}{E} p^\mu f(x, p) \quad (8)$$

where  $f(x, p)$  is the particle phase-space distribution function and  $p^\mu = (E, \mathbf{p})$  is the particle four-momentum vector (we use the signature  $g^{\mu\nu} = \text{diag}(1, -1, -1, -1)$ ). Notice that both  $f(x, p)$  and the combination  $d^3p/E$  are Lorentz scalar invariants. The time-component of  $N^\mu(x)$  is the particle density, while the space-components represent the particle flow, both measured with respect to the observer's frame of reference. By contracting this four-vector with the surface four-vector  $d^3\sigma_\mu$  one can construct the Lorentz scalar

$$\Delta N(x) = \int \int_{\Delta^3\sigma} d^3\sigma_\mu \frac{d^3p}{E} p^\mu f(x, p) \quad (9)$$

Here the time-like four-vector  $d^3\sigma_\mu$  is an oriented three-surface element of a plane space-like surface  $\sigma$ . In the frame where it is purely time-like, expression Eq. (9) reduces to the familiar form for the number of particles in a small volume  $\Delta^3x$  located at  $x$

$$\Delta N(x) = \int \int_{\Delta^3x} d^3x d^3p f(x, p) \quad (10)$$

where  $\Delta^3x$  is a volume element orthogonal to the surface  $\sigma$ . We now introduce the Boltzmann equilibrium distribution function ( $c = \hbar = k = 1$ )

$$f(p) = \frac{1}{(2\pi)^3} \exp\left(\frac{\mu - p^\mu u_\mu}{T}\right) \quad (11)$$

where  $\mu$  is the chemical potential,  $T$  the temperature and  $u_\mu$  the collective fluid or gas four-velocity. Notice that for this integral to converge  $|\mu| \leq m$  and  $u_\mu$  should be time-like (in our metric  $p^\mu$  is time-like and its length positive,  $p^\mu p_\mu = E^2 - \mathbf{p}^2 = m^2$ ). One can now integrate over the whole volume  $V$  and rewrite expression Eq. (10) in the following form

$$\frac{d^3N}{d^3p} = \frac{gV}{(2\pi)^3} e^{(\mu-E)/T} \quad (12)$$

where we have set  $p^\mu u_\mu = E$  (fluid rest frame) and introduced the degeneracy factor  $g$ . The total number of particles  $N$  in the volume  $V$  is thus

$$N = \frac{gV}{(2\pi)^3} e^{\mu/T} \int_0^\infty e^{-E/T} d^3p = \frac{gV}{(2\pi)^3} e^{\mu/T} 4\pi m^2 T K_2(m/T) \quad (13)$$

where  $K_n(z)$  is the modified Bessel function of the  $n$ 'th kind which has the following possible integral representation

$$K_n(z) = \frac{2^{n-1} (n-1)!}{(2n-2)!} \frac{1}{z^n} \int_z^\infty d\tau (\tau^2 - z^2)^{n-3/2} \tau e^{-\tau} \quad (14)$$

and the asymptotic limits

$$K_n(z) \simeq \begin{cases} \sqrt{\frac{\pi}{2z}} e^{-z} & \text{when } z \rightarrow \infty \\ 2^{n-1} (n-1)! z^{-n} & \text{when } z \rightarrow 0 \end{cases} \quad (15)$$

so that the small mass or large temperature limit of Eq. (13) reduces to the familiar Stephan-Boltzmann  $N \sim T^3$  law. Using this equation for  $N$ , one can now renormalize expression Eq. (12), eliminating its dependence on  $e^{\mu/T}$ ,

$$\frac{d^3 N}{d^3 p} = \frac{N}{4\pi m^2 T K_2(m/T)} e^{-E/T} \quad (16)$$

By performing some simple kinematics, remembering that

$$\begin{aligned} E &= m_T \cosh y \\ p_z &= m_T \sinh y \\ y &= \ln((E + p_z)/m_T) \end{aligned} \quad (17)$$

and that  $d^3 p = 2\pi p_T dp_T dp_z = 2\pi m_T^2 dE dy$ , we can now integrate expression Eq. (16) with respect to  $E$  and obtain

$$\begin{aligned} \frac{dN}{dy} &= \frac{N}{2m^2 T K_2(m/T)} \frac{1}{(\cosh y)^2} \int_{m \cosh y}^{\infty} dE E^2 e^{-E/T} \\ &= \frac{N}{2K_2(m/T)} (1 + 2x^{-1} + 2x^{-2}) e^{-x} \end{aligned} \quad (18)$$

where  $x = m \cosh y/T$ .

In Fig. 4 we present a fit to data of Eq. (18) presented by the E802 collaboration<sup>3</sup> for  $^{28}\text{Si} + ^{197}\text{Au}$  at 14.6 A GeV central trigger events. Notice that these data are shifted backwards with respect to nucleon-nucleon center-of-mass rapidity at 14.6 A GeV,  $y_{cm}^{NN} = 1.75$ , whereas the KLM data tended to be approximately centered at  $y_{cm}^{NN}$ . The center of the fit  $y_{fit} = 1.46$  though does not correspond to that expected from a fireball formed by the incident nucleus boring a cylinder with radius  $R = 1.14 A^{1/3}$  through the target nucleus at zero impact parameter, which gives  $y_{cm}^{geom} = 1.25$  (i.e. a fireball made of 28 + 78 nucleons). On the other hand, the difference between the KLM  $\eta_0$  fit parameter and  $y_{cm}^{NN}$  is probably due to the difference between rapidity and pseudorapidity and to the asymmetry between target and projectile; the former tends to make  $\eta_0 > y_{cm}^{NN}$ , whereas the later tends to make  $\eta_0 < y_{cm}^{NN}$ . The KLM "trigger" that  $N_h > 15$ , together with the condition that there are no fragments with  $Z \geq 2$  and  $N_s \geq 208$ , means that there is complete overlap of the oxygen with the target nucleus, so that the effective target-projectile asymmetry in baryon number is probably more like 2 or 3 to 1 (ignoring spectator nucleons), rather than 5 or 7 to 1.

It is interesting to note that in the  $m = 0$  limit, the Boltzmann expression (18) reduces to the isotropic fireball expression (4), which is to be expected since this procedure eliminates all scales from the problem. Another interesting feature of the fits of Fig. 4 is that the kaon curve has a smaller  $\Delta\eta_{FWHM}$  than the pion curve. This is a general feature of the Boltzmann distribution (18), which tends to a delta function in the large mass and fixed rapidity limit.

The fits to the  $K^+$  and  $K^-$  data are not very good and, moreover the temperature parameter  $T = 160$  MeV for kaons, but  $T = 125$  MeV for pions. We thus conclude that

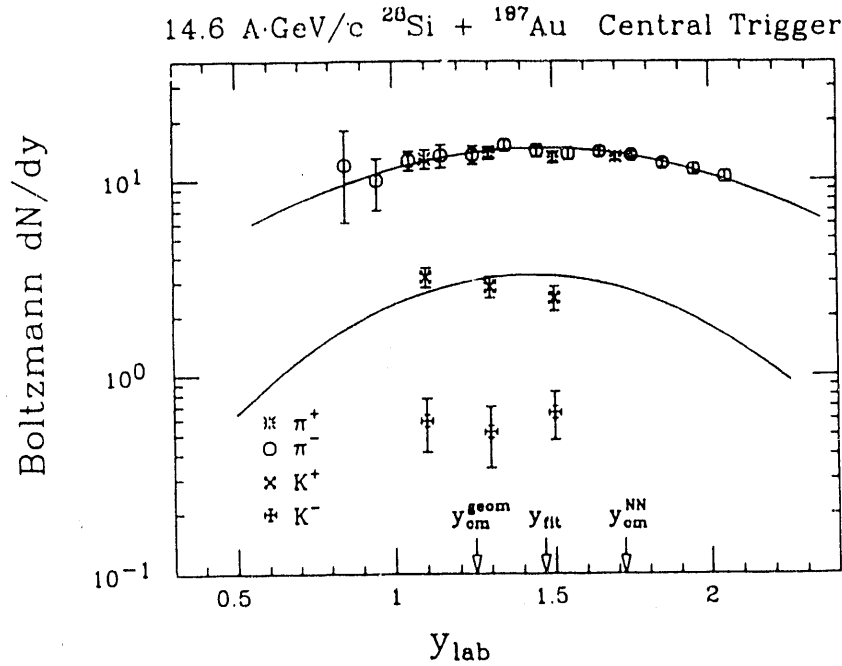


**Figure 4:** Rapidity distribution for Si + Au central collisions at 14.6 A GeV averaged over the number of events.<sup>3</sup> The solid lines are eye fits for a Boltzmann fireball, Eq. (18). Only statistical errors are shown.

this model too is ruled out by experiment. While the  $\pi^+$  and  $\pi^-$  yields are nearly equal, as this model predicts, the  $K^+$  yield is approximately 5 times the  $K^-$ . Several models have attempted to explain this enhancement of strangeness and since it is not observed in pp collisions this may be due to the high energy and/or baryon density achieved in nucleus-nucleus collisions.<sup>9</sup> Clearly, very interesting phenomena are occurring here that lie beyond the ability of this naive model to explain.

Finally, before leaving the subject of  $dN/dy$ , a comparison with pp collisions at the same energy should be mentioned (only meson  $dN/dy$  distributions are discussed here, but recently baryon  $dN/dy$  distributions have also become experimentally available).<sup>10</sup> This comparison was performed for  $^{32}\text{S} + ^{32}\text{S}$  central collisions at 200 A GeV by the NA35 collaboration. They obtain a  $dN/dy$  distribution for negatively-charged particles which peaks at about  $y_{cm}^{NN} = 3.03$  to a value of approximately 30 particles per unit rapidity. It is well approximated by a Gaussian with width  $\sigma = \sqrt{\ln \gamma_{cm}} = 1.53$ , as Landau would have liked. It is also well approximated by rescaling the pp data at the same energy, so that the sulfur + sulfur  $dN/dy \simeq 37.5 * dN/dy|_{pp}$ . The fact that the proportionality factor is larger than 32 probably is due to rescattering effects. The sulfur + sulfur  $\Delta\eta_{FWHM} = 3.2$  and is thus slightly narrower than that for minimum bias 200 GeV pp collisions:  $\Delta\eta_{FWHM} = 3.5$ . Perhaps, for larger colliding nuclei (at the same c.m. energy), this tendency towards narrower widths, approaching the isotropic fireball  $\Delta\eta_{FWHM} = 1.75$ , will continue, contrary to Landau's prediction, in which case, the isotropic fireball model may turn out to be eventually useful. At higher energies a flattening of  $dN/dy$  will probably occur at midrapidity, as observed in pp collisions, and Bjorken's model may turn out to be the appropriate asymptotic scenario.

## II. Flow, entropy and $p_T$ distributions

Clear evidence for the collective phenomenon of flow in heavy ion collisions has been found<sup>11</sup> for  $^{93}\text{Nb} + ^{93}\text{Nb}$  central collisions at 400 A MeV. It was also found that  $^{40}\text{Ca} + ^{40}\text{Ca}$  central collisions exhibit a much weaker flow effect at the same bombardment energy, so that large nuclei, which endure longer as a cohesive whole before the final decoupling into the observed secondaries, were crucial in the conclusive establishment of flow in these reactions. One concludes that to get collective flow one needs a copious amount of rescatterings among the constituent particles of the fireball formed by the collision.

At higher energies pion production dominates the multiplicity and the previous analysis of flow becomes untenable. Nevertheless, the highly excited fireball still has to expand and cool off before it breaks up, since if it breaks up immediately after the collision its temperature and therefore the average transverse momentum  $\langle p_T \rangle$  of the secondaries will be too high to agree with experiment. Moreover, as emphasized by Pomeranchuk,<sup>12</sup> too many heavy particles would be produced without a preliminary expansion. A collective flow should therefore also develop at higher energies in the initial stages of the collision when the constituents of the system are still interacting strongly. The search for evidence of this expected behavior is the main motivation behind this paper and of a series of others.<sup>13</sup>

The observable we will calculate in this search for evidence of flow is the  $p_T$  distribution of the produced secondaries. The data is from the NA35 collaboration<sup>4</sup> and was taken over the central rapidity range  $2 \leq y \leq 3$ , where  $dN/dy$  is approximately constant as we assume in our longitudinal boost invariant hydrodynamics.<sup>14</sup>

The calculation of  $p_T$  distributions starts from Eq. (9) which can be recast in the form

$$E \frac{d^3 N}{d^3 p} = \int_{\sigma} f(x, p) p^{\mu} d^3 \sigma_{\mu} \quad (19)$$

since most produced particles are mesons (90% pions, 10% kaons) the phase space distribution should be the Bose-Einstein

$$f(x, p) = \frac{1}{(2\pi)^3} \frac{1}{\exp(p^{\mu} u_{\mu} - \mu)/T - 1} \quad (20)$$

We now adopt a cylindrical geometry for our fireball which has as initial boundary conditions Bjorken's scaling solution in the longitudinal direction and a zero velocity profile in the transverse direction. The azimuthal symmetry and the scaling solution in the  $z$  direction thus reduce the hydrodynamics from  $3 + 1$  to  $1 + 1$ . The system is now described by the Lorentz invariant independent variables  $z$  (longitudinal direction),  $\tau$  (proper time) and  $r$  (radial coordinate). If we assume a flat rapidity plateau, scalar physical quantities can depend only on  $\tau$  and  $r$ . One is therefore led, by imposing invariance under longitudinal boosts, to the following expression for the fluid four-velocity

$$u^{\mu} = \gamma_r(\tau, r) \frac{t}{\tau} \left( 1, \frac{\tau}{t} v_r(\tau, r), 0, \frac{z}{t} \right) \quad (21)$$

where we have explicitly factored out the longitudinal  $t/\tau$  and radial  $\gamma_r(\tau, r)$  Lorentz factors from the four-velocity, so as to exhibit the transverse  $(\tau/t)v_r(\tau, r)$  and longitudinal components of the fluid velocity. If one now defines the transverse fluid rapidity as

$$\theta = \frac{1}{2} \ln \left( \frac{1 + v_r}{1 - v_r} \right) \quad (22)$$

the expression for the four-velocity, Eq. (21), can be written as

$$u^\mu = \cosh \theta \cosh \alpha (1, \tanh \theta / \cosh \alpha, 0, \tanh \alpha) \quad (23)$$

where  $\cosh \alpha$  is the longitudinal Lorentz factor. Noting that  $dp_z = E dy$  and expanding  $f(p)$ , given by Eq. (20), in a power series and using  $\tau$  and  $r$  as integration variables over the surface  $\sigma$ , Eq. (19) can be written in terms of the Bessel functions  $I_n$  and  $K_n$

$$\begin{aligned} \frac{d^3 N}{dy d^2 p_T} = \frac{g}{2\pi^2} \int_{\sigma} \tau r \sum_{n=1}^{\infty} & \left[ m_T I_0 \left( \frac{np_T \sinh \theta}{T_{dec}} \right) K_1 \left( \frac{nm_T \cosh \theta}{T_{dec}} \right) dr \right. \\ & \left. - p_T I_1 \left( \frac{np_T \sinh \theta}{T_{dec}} \right) K_0 \left( \frac{nm_T \cosh \theta}{T_{dec}} \right) d\tau \right] \end{aligned} \quad (24)$$

where the integral is carried out over the surface  $\sigma$ , defined as the isothermal curve with temperature  $T(\tau, r) = T_{dec} = \text{constant}$ . This decoupling temperature comes from the following considerations. We assume that a hot and non-interacting pion gas is created by the collision, surrounding the fireball, and that its subsequent expansion is governed by hydrodynamics. Initially, the pressure ( $P \sim T^4$ ) will be very high and thus the expansion very fast. At a later stage, after the gas has cooled, the expansion will be quite weak, until eventually the mean free path of the pions becomes comparable to that of the system which then decouples into the free streaming pions observed by the detectors. We assume, as a first approximation, that this occurs at the constant temperature  $T_{dec}$ .

Before proceeding further it is instructive to look at the weak and strong flow limits of Eq. (24). In the case of vanishing radial flow velocity ( $v_r = 0$ ) and  $m_T \gg T_{dec}$  Eq. (24) reduces to the Hagedorn thermal model<sup>15</sup>

$$\frac{dN}{d^2 p_T} = \frac{dN}{d^2 m_T} = A \sqrt{m_T} \exp \left( \frac{-m_T}{T_{dec}} \right) \quad (25)$$

where  $A$  is a constant with respect to  $m_T$ . The NA35 collaboration has fit<sup>4</sup> this expression to the pion spectrum with  $m_T > 0.8$  GeV and to  $K_0$ ,  $p$  and  $\Lambda$  spectra, which were measured only for  $m_T > 0.8$  GeV. For all these particles they get that the parameter  $T_{dec} = 200$  MeV. The low  $p_T$  pions though lie at parameters  $T_{dec} < 200$  MeV. One can therefore rule out the presence of a strong transverse flow in the high  $p_T$  data, but not the presence of a weak transverse flow due to a mixed phase scenario, as we will see shortly. For a strong flow ( $v_r \gg 0$ ) and for  $p_T \gg T_{dec}$ , one can show, using the saddle point method,<sup>15</sup> that Eq. (24) reduces to

$$\frac{dN}{d^2 p_T} = B p_T^{-1/2} \exp \left( \frac{-p_T e^{-\theta_{max}}}{T_{dec}} \right) \quad (26)$$

where  $B$  is a constant with respect to  $p_T$  and  $\theta_{max}$  is the maximum fluid transverse rapidity. Notice now that the temperature is modified effectively by the presence of flow, so that one can define an effective  $T_{eff} = T_{dec} e^\theta = T_{dec} \sqrt{\frac{1+v_r}{1-v_r}} > T_{dec}$  (blue Doppler shifted). Thus a strong collective transverse flow affects the "slope" of the  $p_T$  distributions, when these are plotted on semi-log graphs. One cannot therefore naively interpret these slopes as the temperature of the system. Notice also the different pre-exponential factors in the above two cases, which causes a slight convex curvature for the thermal model and a slight concave one for the strong flow case.

The equation of state we will use in these calculations is a Stephan-Boltzmann gas (non-interacting due to "asymptotic freedom"), with a MIT bag constant (the negative confining pressure of the vacuum), and with the appropriate degrees of freedom for quarks and gluons ( $g_{qq} \simeq 37$ , with half a degree of freedom for the strange quark, to take into account some strangeness content), if the initial energy density exceeds the critical value for quark-gluon plasma formation. If the initial energy density is less than this critical value, the system is in a mixed phase, with a fraction of the matter in the plasma phase and the rest in the pion phase, which is approximated to a Stephan-Boltzmann gas with  $g_\pi = 3$  degrees of freedom.

To estimate the initial energy density one uses the experimentally known total multiplicity per unit rapidity  $dN/dy$  and entropy conservation, as emphasized by Landau. Particle number and entropy are proportional to each other for a massless pion gas since they have the same temperature dependence. Namely, entropy density is given by

$$s_\pi = 3 \frac{4\pi}{90} T^3 \quad (27)$$

and particle number density by

$$n_\pi = 3 \int_0^\infty \frac{d^3p}{(2\pi)^3} \frac{1}{e^{p/T} - 1} = \frac{3 \zeta(3)}{\pi^2} T^3 \quad (28)$$

so that  $s_\pi = 3.6 * n_\pi$ . Therefore,  $dS/dy|_{final} \simeq 3.6 dN/dy$  and if entropy is conserved as in Bjorken's model  $dS/dy|_{initial} = \pi R^2 \tau_0 s_0 = \pi R^2 \tau_f s_f = dS/dy|_{final}$  (where  $R$  is the nuclear radius,  $\tau_0$  the initial formation proper time and  $s_0$  the initial entropy density, while  $\tau_f$  and  $s_f$  are the corresponding final quantities) one finds that

$$s_0 \simeq \frac{3.6}{\pi R^2 \tau_0} \frac{dN}{dy} \quad (29)$$

Entropy conservation thus provides us with a window into the earlier stages of the collision.

The NA35 data for  $^{32}\text{S} + ^{32}\text{S}$  collisions at 200 A GeV has a  $dN/dy \simeq 30$  at mid-rapidity ( $y = 3.03$ ) for negatively charged particles (90% pions), so that the total  $dN/dy \simeq 90$ . Assuming  $\tau_0 = 1.25$  fm/c and  $R = 3.5$  fm, one finds from Eq. (29) that  $s_0 = 6.7 \text{ fm}^{-3} = g_\pi (4\pi^2/90) T^3$ , which gives  $T \simeq 334$  MeV ( $g_\pi = 3$ ) and initial energy density  $\epsilon_0 = \frac{3}{4} s_0 T \simeq 1.6 \text{ GeV/fm}^3$ . This temperature is barely consistent with even a super-heated pion gas and for values larger than this the system cannot be considered an ideal gas since interactions cannot be neglected when the density of the gas is comparable to that of one pion (extra hadronic resonances

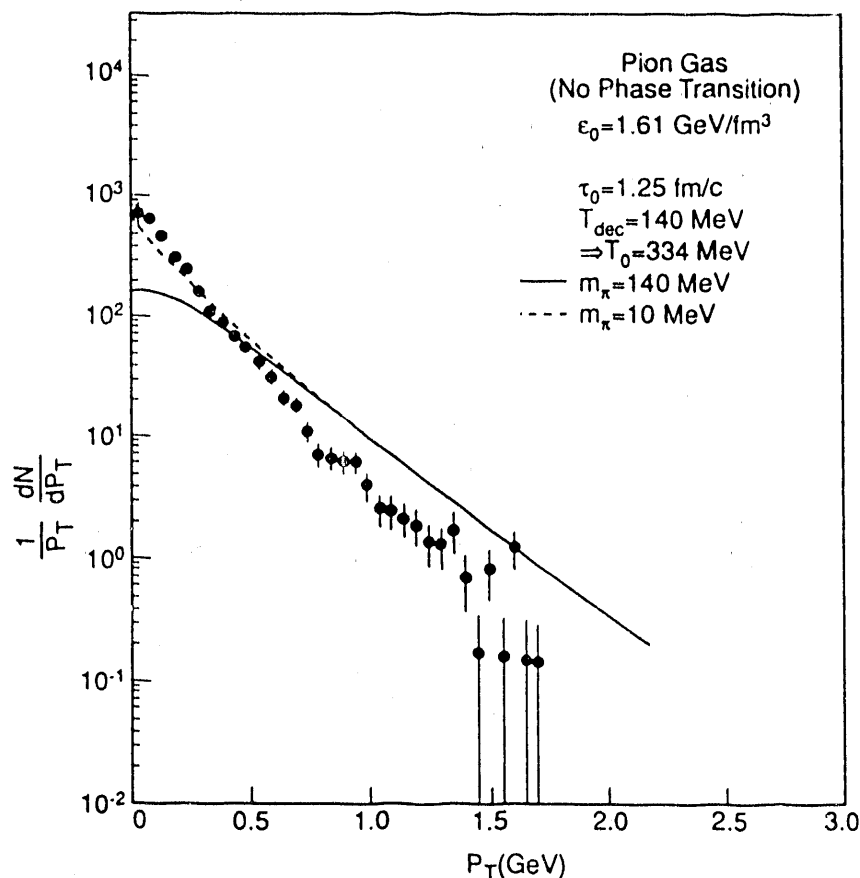


**Figure 5:** The  $p_T$  distribution for a pion gas and the NA35 S + S preliminary data for negatively charged particles at 200 A GeV.

resonances like  $\rho$ ,  $\omega$  and  $\eta$  must be included, thereby increasing the number of degrees of freedom and reducing the initial temperature of the gas).

Keeping in mind the above caveats, we plot in Fig. 5 the  $p_T$  distribution calculated with the above initial conditions supplemented with a decoupling temperature  $T_{dec} = 140$  MeV and compare it to the preliminary NA35  $^{32}\text{S} + ^{32}\text{S}$  data. Notice the slight positive curvature of the distribution in the range  $0.5 \text{ GeV}/c < p_T < 2.0 \text{ GeV}/c$  and the large difference between the massive and massless cases. At high  $p_T$  the pion mass is comparatively small so that the two scales coincide. Integrating the curve for the massless case  $dN/dy = 91$  and the  $\langle p_T \rangle = 455 \text{ MeV}/c$ , so that the pion gas assumption underestimates the contribution of the low  $p_T$  component of the distribution and overestimates the high  $p_T$  component.

If, instead of a pure pion gas, a first order phase transition to a quark-gluon plasma occurs at  $T_c = 160$  MeV, the critical entropy density for the pion and quark gluon phases are:  $s_\pi(T_c) = 0.704 \text{ fm}^{-3}$  and  $s_{qg}(T_c) = 8.6 \text{ fm}^{-3}$ . The initial high density state formed by the  $^{32}\text{S} + ^{32}\text{S}$  collisions at 200 A GeV is thus a mixed phase of pions and quark-gluon plasma. From the equation  $6.7 = 0.704(1 - f) + 8.6f$ , we obtain the fraction of the matter that is in the quark-gluon plasma phase,  $f = 76\%$ . The initial energy density can now be calculated:  $\epsilon_0 = \epsilon_\pi(1 - f) + \epsilon_{qg}f$ , where  $\epsilon_\pi = 0.084 \text{ GeV}/\text{fm}^3$  and  $\epsilon_{qg} = 1.03 \text{ GeV}/\text{fm}^3$ , which

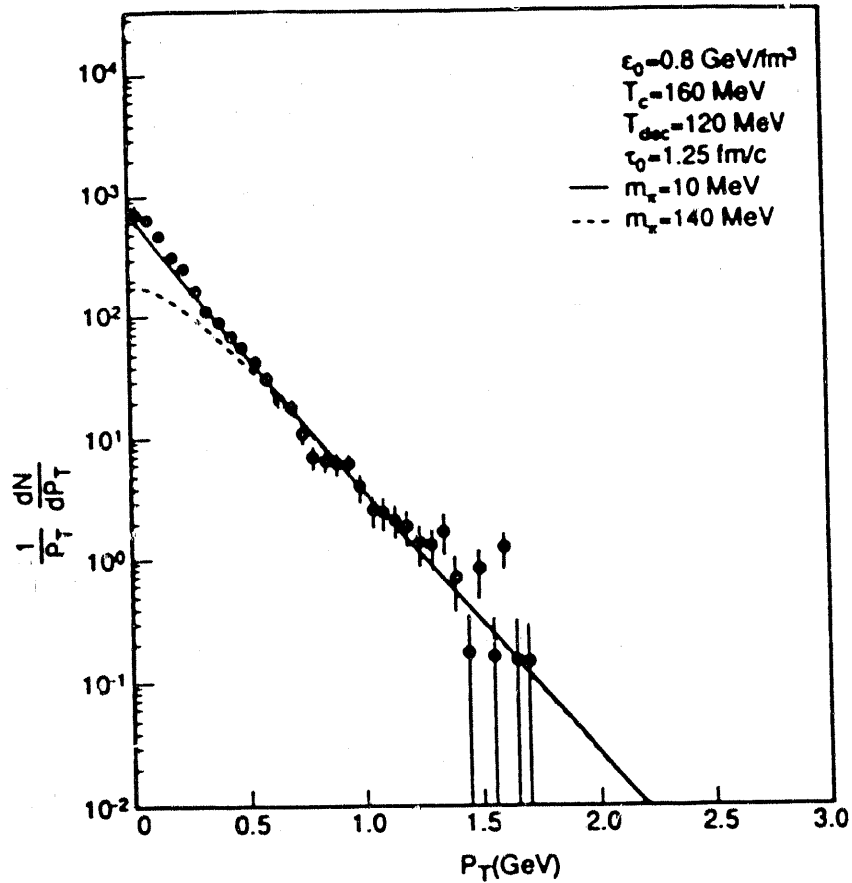


Figure 6: The  $p_T$  distribution for a mixed phase scenario.

results in  $\epsilon_0 = 0.8 \text{ GeV/fm}^3$ . In Fig. 6 we show the  $p_T$  distribution one finds assuming these initial conditions and a decoupling temperature of  $T_{dec} = 120 \text{ MeV}$ . For the massless case ( $m_\pi = 10 \text{ MeV}$  to avoid divergences in the decoupling integral)  $dN/dy = 75$  and  $\langle p_T \rangle = 330 \text{ MeV/c}$ , whereas the experimental values are total  $dN/dy = 3 \times 28 = 84$  and  $\langle p_T \rangle = 350 \text{ MeV/c}$ . When the pion mass is included a disagreement of almost an order of magnitude with the data is found at low  $\langle p_T \rangle$ , where the bulk of the multiplicity resides (in the NA35 data 76% of the charged particles observed have  $p_T < 500 \text{ MeV/c}$ ). The enhancement of the low  $p_T$  component for the massless case is due to the singular behavior of the Bose-Einstein distribution in the decoupling integral in the limit when  $p_T$  and  $m_\pi$  vanish. The striking feature of this curve is its complete lack of curvature, except at very low  $p_T$  values. Compared to the pure pion gas, a much softer flow is now generated. This is due to the mixed phase which causes the system to last longer (the velocity of sound vanishes), thus making it more susceptible to the  $p_T$  attenuating effects of the longitudinal expansion. A suppression of strong transverse flow effects is thus obtained.

Before concluding we mention some of the shortcomings of the calculations presented here: they assume zero impact parameter and equal  $A$  colliding nuclei for all events (no multiplicity or energy fluctuations are put into the individual event generated). In addition, Bjorken's longitudinal scaling solution is used throughout the systems expansion (note that

Landau's model also obtains the same scaling solution for short times, when the transverse dimensions of the system can be neglected) and the phase transition is assumed to occur smoothly. Finally, truly three-dimensional hydrodynamical calculations with a finite longitudinal extent, capable of incorporating phenomenologically the strong stopping observed at these energies, and with more realistic equations of state, that include viscosity and temperature dependent velocity of sound effects, should be carried out.<sup>13</sup>

In conclusion we emphasize the following points: (i) Rapidity and pseudorapidity distributions are approximately Gaussian in shape for energies in the range 14.6 to 200 A GeV. The widths increase monotonically with beam energy, but are essentially independent of the multiplicity at a fixed beam energy. Quantitatively, the widths are consistent with Landau's hydrodynamical model and inconsistent with the an isotropic fireball and Bjorken's hydrodynamical scaling model. A Boltzmann model seems to be consistent with the pion rapidity distribution at 14.6 A GeV, but is inconsistent with the kaon data. The distributions are also not centered at the rapidity one would expect from a fireball formed by the projectile boring a cylindrically excited region through the target. From this failure of the isotropic model, one can conclude that an ellipsoidal momentum configuration is more appropriate than a spherical one in describing events at these energies. (ii) A non-zero collective flow velocity tends to give transverse momentum distributions a concave shape for effectively massless particles. (iii) An ideal pion gas is ruled out by the data since it generates too strong a transverse flow. (iv) The presence of a mixed phase in the equation of state tends to soften the transverse flow, leading to lower values of the  $\langle p_T \rangle$  as compared to the ideal pion gas case. On a semi-log plot these distributions have a linear behavior for a large  $p_T$  range and are thus nearly indistinguishable from the thermal model ones, which have zero flow velocity.<sup>15</sup> (v) The non-zero slope of the experimental  $p_T$  distribution at small  $p_T$  values cannot be understood solely within the framework of relativistic hydrodynamics. Some new physics is needed here (note that we have ignored entirely the role of nucleons and of interactions among the constituent particles in these models). (vi) No unambiguous evidence for collective flow has emerged from our analysis. Perhaps this will only happen when higher energies and heavier nuclei become available at CERN and RHIC.

## REFERENCES

1. For a review of the field see the Proc. of the VII'th Int. Conf. on Ultrarelativistic Nucleus-Nucleus Collisions, Lenox, U.S.A., edited by G. Baym, P. Braun-Munzinger and S. Nagamiya, Nucl. Phys. **A498** (1988).
2. H. von Gersdorff *et al.*, Phys. Rev. **C39** (1989) 1385.
3. O. Hansen, Proc. of the Int. Workshop XVIII on Gross Properties of Nuclei and Nuclear Excitations, Hirschegg, Austria (1990);  
M. Tannenbaum, Proc. of the Workshop on Heavy Ion Physics at the AGS edited by O. Hansen (1990) 44.
4. J. W. Harris, ref. 1, pg. 133c;  
G. Odyniec, Proc. of the Int. Workshop on Relativistic Aspects of Nuclear Physics, Rio de Janeiro, Brasil, edited by T. Kodama (1989).
5. J. D. Bjorken, Phys. Rev. **D27** (1983) 140.

6. L. D. Landau, *Isv. Akad. Nauk SSSR, Ser. Fiz.* 78 (1953) 51; *Collected Papers of L. D. Landau*, edited by D. Ter Haar (Pergamon, Oxford, 1965), 569.
7. S. DasGupta and A. Z. Mekjian, *Phys. Rep.* 72 (1981) 131.
8. S. R. de Groot, W. A. van Leeuwen and Ch. G. van Weert, *Relativistic Kinetic Theory*, (North-Holland Publ., 1980).
9. P. Koch, B. Müller and J. Rafelski, *Phys. Rep.* 142 (1986) 167.
10. J. Costales, *Proc. of the Workshop on Heavy Ion Physics at the AGS* edited by O. Hansen (1990) 249.
11. H. A. Gustafson *et al.*, *Phys. Rev. Lett.* 52 (1984) 1590.
12. I. Ya. Pomeranchuk, *Dokl. Akad. Nauk SSSR* 78 (1951) 889.
13. E. F. Staubo, A. K. Holme, L. P. Csernai, M. Gong and D. Strottman, *Phys. Lett.* B229 (1989) 351;  
K. S. Lee, U. Heinz and E. Schnedermann, Regensburg preprint (1990) to appear in *Z. Phys. C*;  
R. Venugopalan and M. Prakash, *Phys. Rev.* C41 (1990) 221;  
U. Ornik, F. Pottag and R. Weiner, *Phys. Rev. Lett.* 63 (1989) 2641;  
D. Kusnezov and G. Bertsch, *Phys. Rev.* C40 (1989) 2075.
14. P. V. Ruuskanen, *Z. Phys.* C38 (1988) 219.
15. J.-P. Blaizot and J.-Y. Ollitrault, *Nucl. Phys.* A458 (1986) 745;  
P. V. Ruuskanen, *Acta Phy. Polon.* B18 (1987) 551.

#### DISCLAIMER

This report was prepared as an account of work sponsored by an agency of the United States Government. Neither the United States Government nor any agency thereof, nor any of their employees, makes any warranty, express or implied, or assumes any legal liability or responsibility for the accuracy, completeness, or usefulness of any information, apparatus, product, or process disclosed, or represents that its use would not infringe privately owned rights. Reference herein to any specific commercial product, process, or service by trade name, trademark, manufacturer, or otherwise does not necessarily constitute or imply its endorsement, recommendation, or favoring by the United States Government or any agency thereof. The views and opinions of authors expressed herein do not necessarily state or reflect those of the United States Government or any agency thereof.

**END**

**DATE FILMED**

12 / 27 / 90

